sciendo

Original Study

Open Access

Michał Siegmund*, Marek Kalita, Dominik Bałaga, Krzysztof Kaczmarczyk, Józef Jonak

Testing the rocks loosening process by undercutting anchors

Abstract: The method of unconventional solid rock loosening with undercutting anchors and the literature analysis of the problem are presented. The tests and test results of the rocks loosening process with a fixed undercutting anchor are described. The tests were carried out within the RODEST project, OPUS 10 competition No. 2015/19/B/ST10/02817, financed by the National Science Centre. Numerical modeling process as well as a series of laboratory and in situ tests were carried out. The test stand equipment and methodology for the in situ tests are presented. The tests were conducted in four mines, which allowed to obtain and determine the following characteristics:

1. loosening force as a function of anchoring depth (for a given type of rock),
2. the range of rock loosening in a function of anchoring depth (for a given type of rock), and
3. loosened rock volume as a function of anchoring depth (for a given type of rock).

The in situ test results are compared with the concrete capacity design (CCD) model used for the calculation of anchor load capacity in concrete.

Keywords: destroying the integrity of rocks; tearing out rock fragments; mine rescue operations; unconventional rock cutting; rock strength tests.

*Corresponding author: Michał Siegmund, KOMAG Institute of Mining Technology, Pszczyńska 37, 44-100 Gliwice, Poland, E-mail: msiegmund@komag.eu
Marek Kalita, Dominik Bałaga, Krzysztof Kaczmarczyk, KOMAG Institute of Mining Technology, Pszczyńska 37, 44-100 Gliwice, Poland
Józef Jonak, Lublin University of Technology, Faculty of Mechanical Engineering, Nadbystrzycka 36, 20-618 Lublin, Poland

1 Introduction

Taking into account the specific conditions prevailing in mining roadways, it should be noted that the mining process is both time and energy consuming. Excavation of solid rocks belongs to one of the most difficult mining processes due to its multistage character and technological diversity. Development of roadways in the Polish hard coal mining industry is carried out either with roadheading machines or using explosives [17]. The energy consumption criterion largely determines the final costs of the technology. It is not conducive to introducing new, innovative solutions in the mining industry that meet the mentioned criterion. This problem is particularly frequent at the stage of implementing new technologies. Many design solutions of machines and devices, as well as of new technologies, are difficult to be implemented despite the positive results obtained during surface stand tests. Rescue operations are the situations when economic issues no longer have a decisive impact on the drilling technology, but are only the practical issues [20]. Searching for alternative methods to the known rock mining methods (mechanical and blasting) is needed to limit the emission of gases harmful to health and environment as well as to limit the use of mechanical mining technologies near important buildings and industrial installations (e.g. due to generated vibrations). Only manual mining applying lightweight pneumatic hammers is often used in such cases. However, this is inefficient and time consuming [4].

The technology of destroying the integrity of rocks using undercutting anchors fixed in the walls [16] is an alternative method developed by KOMAG in several variants.

The method of mechanical rock loosening is based on drilling holes in the face of a mined working, into which the pulling rods with expanding parts are inserted (Figure 1). The force P acting on the pulling rod (3) anchored in the rock with an expansion sleeve (4) causes it to detach (2) from the rock mass (1) [4, 16, 20].

This method is safe because it does not pose any hazard related to burst of blasted rock and can be used
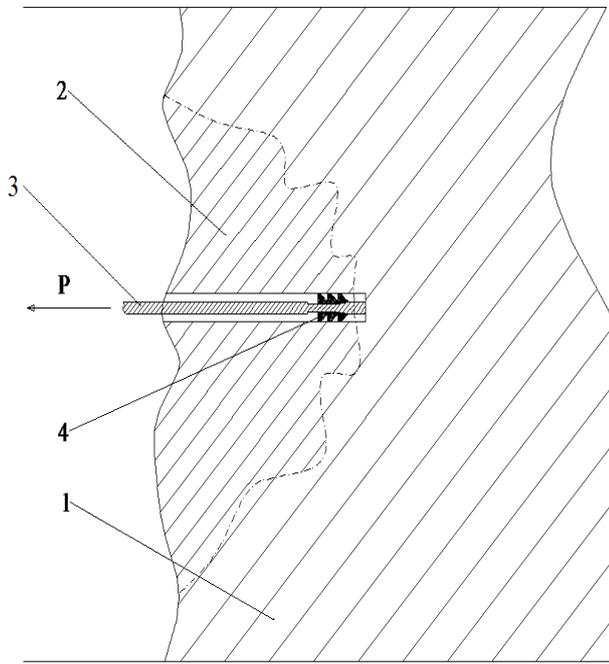
Figure 1: The concept of cutting the solid rock through destruction of its integrity: 1. solid rock, 2. loosened rock, 3. pulling rod, 4. expansion sleeve [4, 16, 20].

Figure 2: Different failure mechanisms of cast-in and post-installed mechanical anchors [2].

regardless of the level of methane hazard. This technology does not cause destruction of the rock mass outside the strictly defined zone, and in no way affects the surrounding environment (no gas emission or generated vibrations) [4, 16, 20].

The problem of loosening (mining) using the undercutting anchors has not been investigated so far, both in the Polish and global industry. The state of the art in the subject of applying the anchors concerns mainly the fastening systems used in the assembly of industrial infrastructure in engineering-reinforced concrete structures. Stress condition of the rock, generated by the force applied to the pulling rod fixed with an expansion sleeve, can be referred to as the load-bearing capacity of mechanical anchors. Generally, five failure mechanisms are identified [1, 5, 6, 7]. As shown in Figure 2, these failure mechanisms are as follows:

✓ steel failure (Figure 2a),
✓ concrete cone failure (Figure 2b),
✓ bursting failure(Figure 2c),
✓ pull-out failure (Figure 2d), and
✓ concrete splitting failure (Figure 2e).

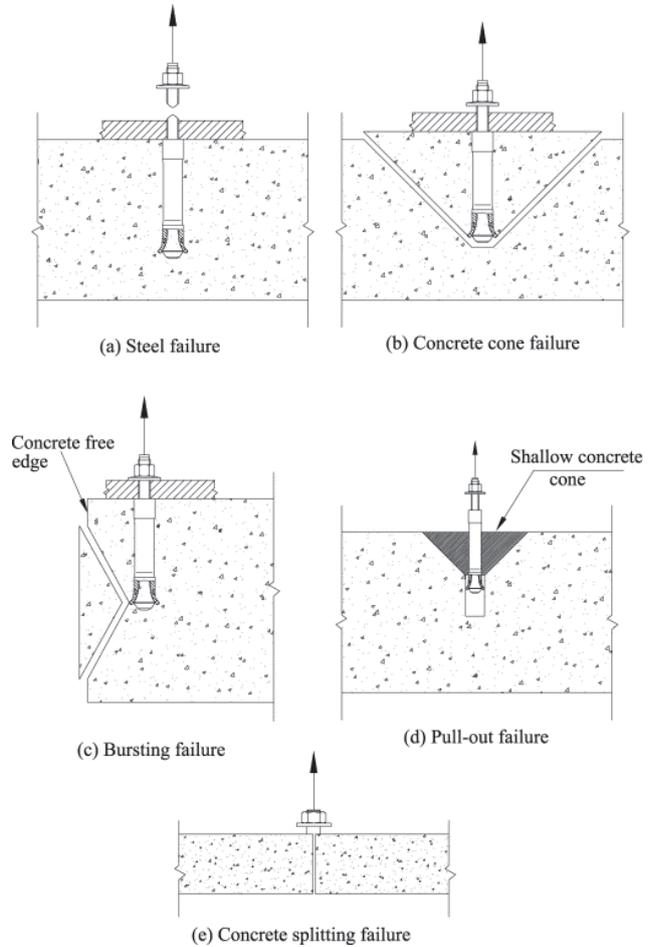Method of cutting the solid rock with an undercutting anchor can be compared to the problem of damaging the anchor connection by tearing out the concrete cone (Figure 2b). The scientific literature [2, 9, 18, 23] cites several methods for calculation of anchor tensile capacity, corresponding to the failure caused by concrete cone tear out. Most of these approaches are similar and each uses two main variables: the anchoring depth H_{ef} and the concrete compressive strength f_c, as an index of the concrete tensile strength.

There are two most commonly used methods for estimation of anchor fixation resistance to failure caused by concrete cone tear out, i.e. the 45° cone failure method and the method for computational concrete capacity design (CCD). In the case of the 45° cone method, the concrete is assumed to form a conical surface around the steel–concrete connector with an angle of approximately 45° (as shown in Figure 3a) measured between the surface perpendicular to the anchor axis and the cone surface [9].

A constant distribution of tensile stresses is then assumed. The concrete cone failure load $N_{u,m}$ of a single
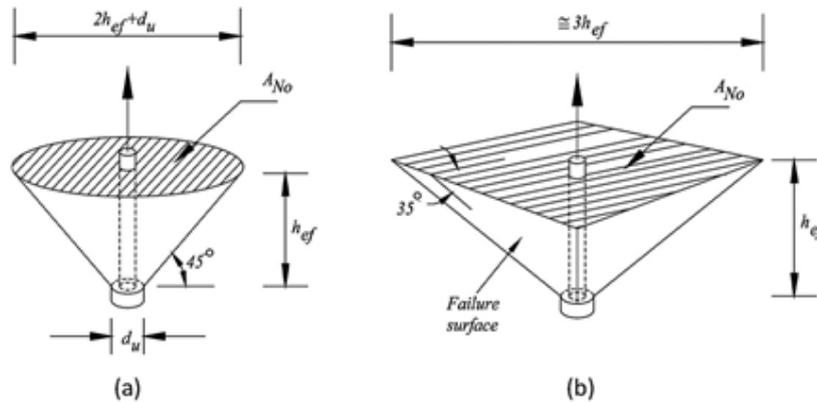
Figure 3: Base material failure models according to: a) ACI 349-85 (conical failure) and b) CCD (four-sided pyramid failure) [2, 9, 22, 23] CCD, concrete capacity design.

anchor in uncracked concrete unaffected by edge influences or overlapping the cones of neighboring anchors is given by [9]:

$$N_{u,m} = 0.96\sqrt{f_{cc}}H_{ef}^2 \left(1 + \frac{d_h}{H_{ef}}\right) \qquad (1)$$

where: $N_{u,m}$ – mean anchor load capacity (N); f_{cc} – concrete compression strength measured on cubes (N/mm²); H_{ef} – effective embedment depth (mm); d_h – mean anchor head diameter (mm).

The second CCD method assumes a similar destruction mode with one exception: the pull-out has the form of a four-sided pyramid with an angle of damage of 35° between the concrete component and the loosened rock surface, as shown in Figure 3b [9]. The concrete cone failure load $N_{u,m}$ of a single anchor in uncracked concrete unaffected by edge influences or overlapping cones of neighboring anchors is given by [9]:

$$N_{u,m} = k\sqrt{f_{cc}}H_{ef}^{1.5} \qquad (2)$$

where: $N_{u,m}$ – mean anchor load capacity (N); k – calibration factor (13.5 for post-installed fasteners, 15.5 for cast in situ headed studs and headed anchor bolts); f_{cc} – concrete compression strength measured on cubes (N/mm²); H_{ef} – effective embedment depth (mm).

In the context of loosening range, practice shows that these are oversimplifications. The angles at the base of the cone in reality are almost 2 times smaller than the standard ones, which is the reason that the estimated ranges of the loosening, and hence the volume of the

loosened rock mass, are significantly understated. The real loosening ranges (crack propagation) in the light of the few literature items [3, 12, 19, 23] are shown in Figure 4.

The models developed and used so far allow forecasting the anchor load capacity in a concrete block with high accuracy. However, the problem of fixing in rocks in a "raw" rock mass and not, e.g. in a concrete housing, is still insufficiently tested, especially due to the extent of the loosening gap.

That is why, in order to assess the potential application of the rock cutting method with the use of anchors, it is extremely important to determine the loosening range depending on the depth of effective anchoring and the rock strength, as this significantly affects the volume of the loosened rock, which in turn affects, e.g. the process energy consumption.

2 Testing the process of loosening the rocks using the undercutting anchors

In order to fully understand the mechanism of loosening and strain in the pulled out rock, realization of the RODEST project entitled "Research and modelling of the mechanism for destruction of rock materials in the spatial state of shear and tensile stress" was undertaken. The project is realized by the scientific consortium: KOMAG Institute of Mining Technology together with the Lublin University of Technology and is financed by the National Science Centre as part of the OPUS 10 competition (project no. 2015/19/B/ST10/02817) [15].
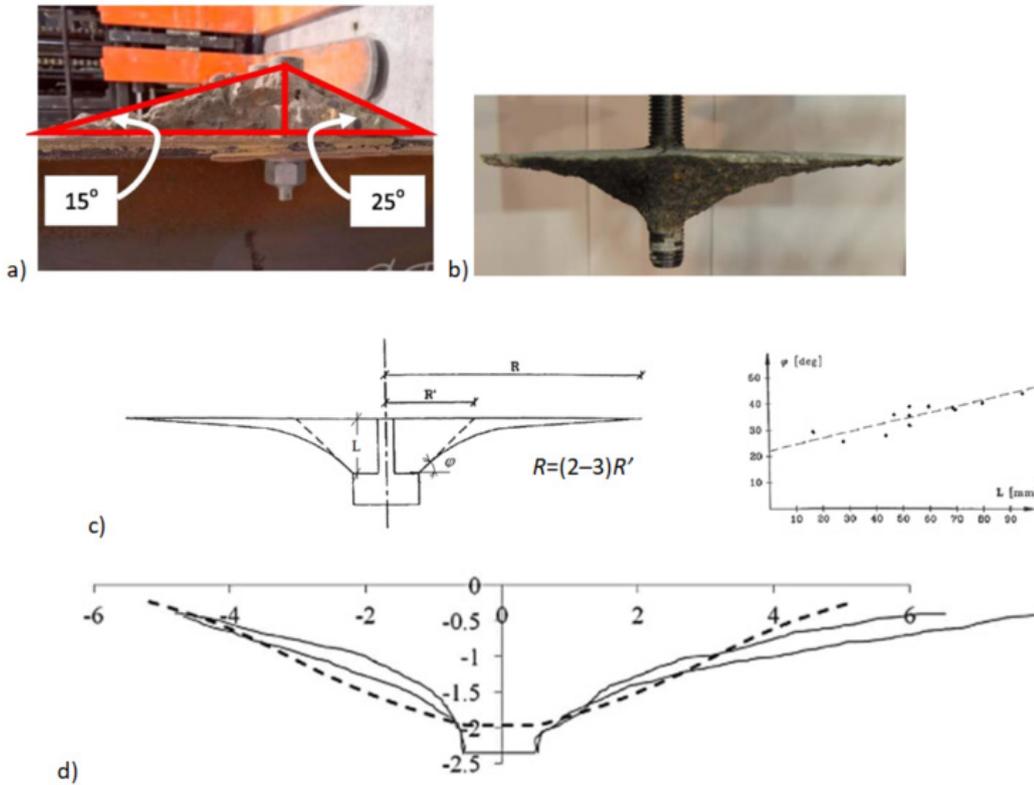
$$R=(2-3)R'$$

Figure 4: Real extent of the loosening process based on literature data: a, b) concrete cone [12, 23]; c) radius *R* observed by test and effective radius *R'* used in model [3]; d) comparison between LEFM predictions (dashed lines) and experimental crack propagation patterns [19]. LEFM, linear elastic fracture mechanics.
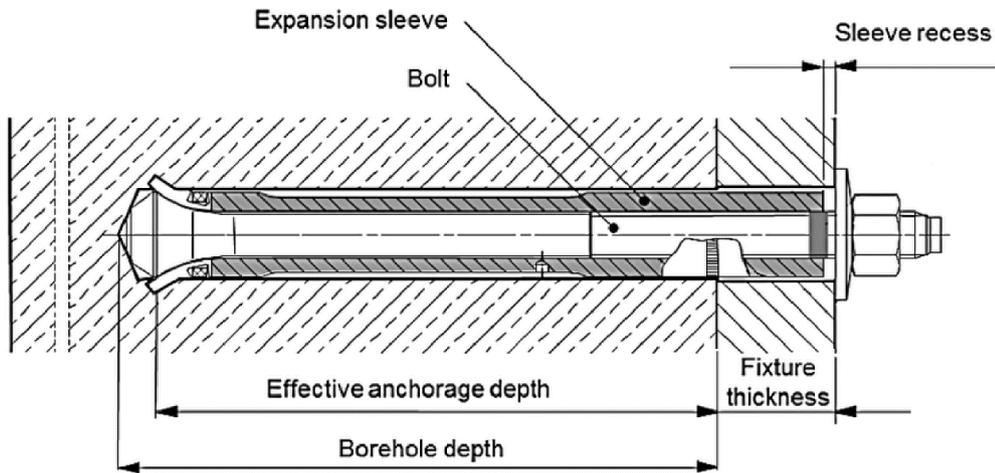

Figure 5: An example of the undercutting anchor [13].

In the project series, in situ tests and numerical simulations were conducted. The tests enabled to gain new knowledge about the process of rocks' destruction under load from the undercutting anchor.

2.1 Undercutting anchor

The experience of KOMAG in the field of rock cutting tests with the use of mechanical anchors clearly shows that for this method, due to the nature of the applied loads, the
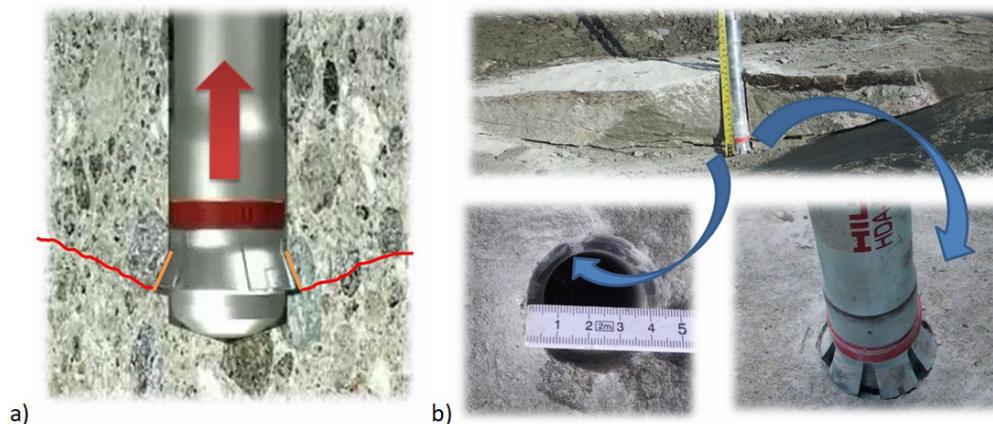
Figure 6: Loosening process with use of an undercutting anchor: a) line of crack propagation, b) fixation method.

most reasonable is to use the undercutting anchors [8]. The legitimacy of using undercutting anchors is due to the way the stress is exerted by the anchor, where all the stress caused by the applied force is concentrated at the place of the shaped undercut at the bottom of the hole. Figure 5 shows an example of the undercutting anchor manufactured by HILTI [13].

Setting this type of anchor consists of placing it in a previously prepared hole of the required depth. Then, using a hammer drill and a special device, torque and axial force from the impact act on the expansion sleeve. Such load to the anchor sleeve causes it to expand on the conical end of the anchor while undercutting the bottom hole. After loading the anchor with an axial force directed to the hole bottom, the force begins to act on the walls of the undercut, which, after exceeding the critical value, creates a crack and causes its propagation. The mechanism of fixation of the undercutting anchor in the rock through a shaped joint with the marked place of application of the loosening force is shown in Figure 6a. In turn, Figure 6b shows an example of the crack progress during rock loosening process, together with an illustration of the undercut residues at the beginning of its propagation.

In all tests carried out within the RODEST project, anchors of the same anchoring mechanism, i.e. by undercutting, were used. The anchors used during the tests were HILTI HDA-P undercutting anchors with nominal size M20 (Figures 5 and 6).

2.2 Numerical tests using finite element method

Also, the computer simulation tests carried out so far using the finite element method (FEM) do not give an unequivocal answer regarding the range of propagation of the crack during rock loosening. It is necessary to compare different methods of crack propagation with the in situ tests to check their accuracy. The numerical analysis was carried out using the FEM ABAQUS system [14]. The 3D model was obtained by rotating a flat model (Figure 7a) around the longitudinal axis of the anchor. This model was discretized with C3D8R elements (linear, continuum 3D element, eight-node reduced integration). The impact of the anchor head (conical part) on rock was modeled in a simplified way by applying vectors of elemental forces in the nodes of the surface of hypothetical contact of the anchor with rock. The tests indicate that for the assumed mechanical parameters of rock and the depth of undercutting the rock with an anchor, the value of the angle of the cone failure is approximately 25º (Figure 7b) [14]. Figure 7c illustrates the numerically obtained failure (cracking) surface and distribution of maximal principal stresses. The crack near the top edge began to distort and return. This is related to the limitations of ABAQUS procedures. The state of stress here was so complex that the program probably could not decide how to lead the crack. For various program settings and different meshes, it was not possible to cause the crack to go through to the end. Details of numerical analyses of the impact of a single anchor and the results obtained are presented in the papers [10, 11, 14].
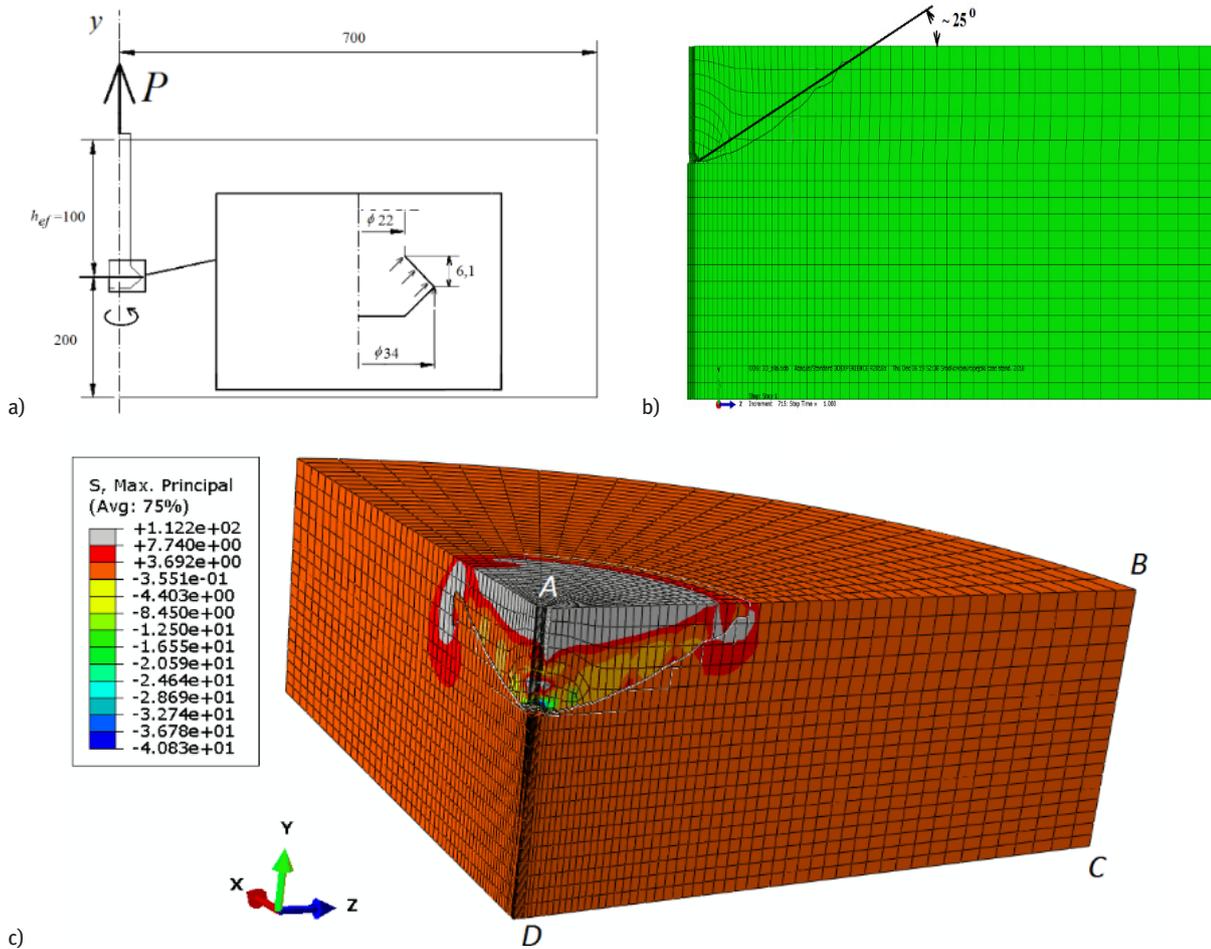
Figure 7. Computer simulations [14]: a) scheme of the task, b) the average value of the angle of the concrete cone failure (section plane ABCD in Figure 7c), c) maximal principal stress distribution and crack propagation path in the FEM model (a quarter of the model). FEM, finite element method.

2.3 Test stand in in situ conditions

The test stand for the rock loosening tests required development of a prototype testing device enabling in situ tests. Therefore, it was necessary for the test stand to have a simple and reliable structure, enabling manual transport, assembly, and operation. Design of the testing device was adapted to each testing condition. The arrangement of the testing device for the loosening test is shown in Figure 8.

The cylinder support (1) enables proper support of the test cylinder (2) expanding the pulled out anchor. The support allows the use of two types of pull-out cylinders (30 and 60 T) interchangeably by using the special connection plate. At the same time, the component provides support against solid rock at three points located at a diameter of 1 m. At each supporting point, there is the possibility of adjusting (adjustment in the range of 0–180

mm) the support point to the unevenness of the operating front by tightening the pressure clamps. Pressure clamps also enable coaxial positioning of the cylinder (2) with a previously embedded anchor in the rock (4). By using the pressure recorder (5) and known active surface of the cylinder (2), it is possible to obtain the time process of changes in the pulling force during the loosening test. The test stand equipment is complemented by an auxiliary equipment enabling efficient testing of and recording the parameters, their changes, and the results of loosening tests. Additional equipment components include: a hammer drill with accessories, a manual hoist, and clamping ropes or a set of tools. The tests were recorded using a video camera, while the loosening measurements were taken using the hand-held measuring instruments and a hand-held 3D scanner.
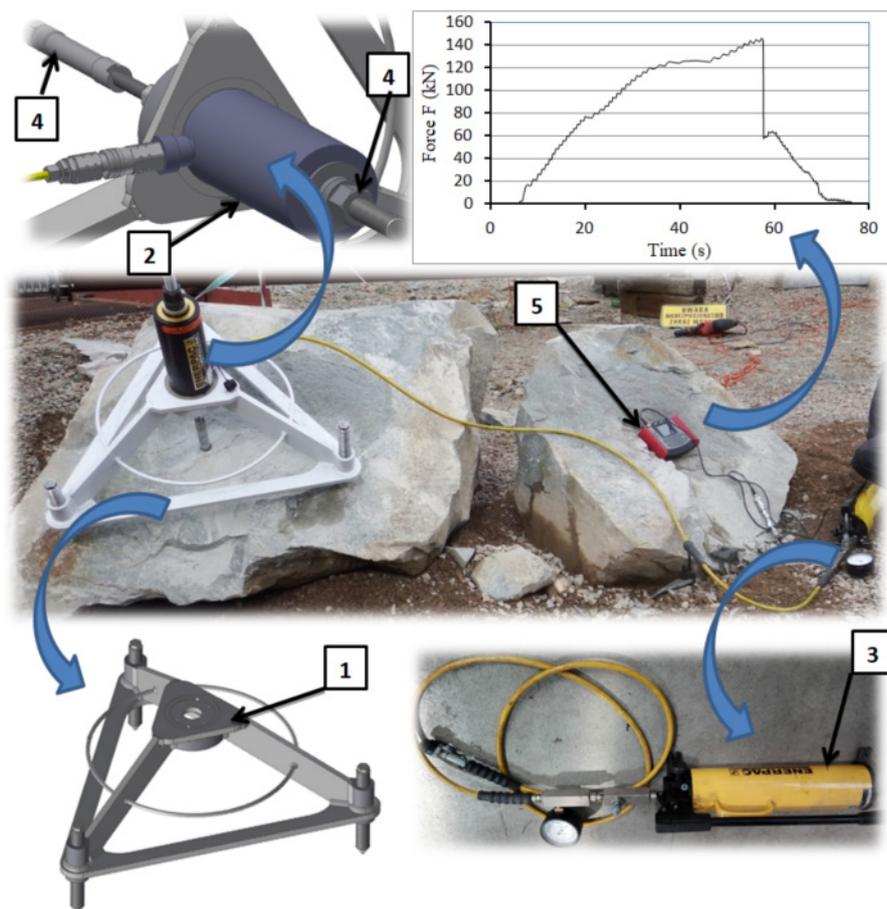
Figure 8: The RODEST test stand equipment As a standard, the testing device is equipped with the following components (Figure 8):
1. cylinder support,
2. hydraulic cylinder with a cylindrical through hole,
3. supply unit (hand pump + hoses, pressure gauge, connectors),
4. undercut anchor with fastening equipment, and
5. supply pressure recorder.

2.4 Place of tests

Tests of loosening the rocks from a solid rock, due to the necessity of diversification of rock strength properties, were carried out for four different types of rocks in the following four mines:
1. The ZALAS open-cast porphyry mine: The tests were conducted on large, not damaged rock blocks separated in the result of mining with explosives (Figure 9a).The tested rocks can be classified as magma rocks of a porphyry structure.
2. The BRACISZÓW open-cast sand mine: The tests were conducted on large, not damaged rock blocks separated in the result of mining with explosives (Figure 9a).The tested rocks can be classified as a graywacke sandstone occurring in Góry Bardzkie and East Sudeten mountains.

3. GUIDO hard coal mine: The tests were carried out at the level of 320 m, at the longwall, on the mining front made in sandstone (Figure 9c). The tested rocks can be classified as fine and medium grain sandstones of Upper Silesian Coal Basin (USCB).
4. The BRENNA open-cast sand mine: The tests was carried out on the mining front of the oblique stratified rock (Figure 9d). The tested rocks can be classified as Godula Sandstones in the Skoczów area.

Each time, the rock material was collected from the testing site for the laboratory tests. In the laboratories of the Department of Geomechanics and Underground Construction of the Faculty of Mining and Geology of the Silesian University of Technology, strength tests of the material delivered by the KOMAG Institute of Mining Technology in Gliwice were carried out. The tests were

Figure 9: Place of tests: a) ZALAS, b) BRACISZÓW, c) GUIDO, d) BRENNA.

carried out in accordance with the suggestions of the International Society of Rock Mechanics (ISRM), meeting the recommended standards regarding the sampling accuracy, used instruments, and the testing method. Shaped, cylindrical samples of diameter d = 42 mm and of various slenderness ratios h/d were prepared for the tests. Uniaxial compression tests and tensile tests by the Brazilian method were carried out.

Measurement consistency c and angle of internal friction j for the tested rocks were determined in shear under compression tests. Shear force in shear under compression tests for the set shear angles 15° and 30° was measured to determine the maximum normal stresses $s_{n\max}$ and tangential stresses $t_{t\max}$. Based on these stresses determined in four tests, the following Coulomb limit state equation was developed:

$$\tau = \sigma \tan(\varphi) + c \qquad (3)$$

where: t – shear strength; s_n – normal stresses; φ – angle of internal friction; c – cohesion.

The mean values calculated from the test results are presented in Table 1.

2.5 Scanning of the loosening surface

In order to obtain the dimensions of detached rock cones, during the tests, the loosening surfaces were scanned with the use of the hand-held 3D scanner. As a result of the scan, a cloud of points was obtained, which after initial manual processing were converted into an STL (stereolithography) triangle mesh. In the specialized LEIOS 2 software, the STL model was processed and converted to the .sat model. Using a solid 3D model in Autodesk Inventor, a derivative in the form of a detached cone was developed. The processing of scans is shown in Figure 10 [21] in a schematic way.

Figure 10: Scheme of processing the scans of rocks surfaces after their loosening.

Table 1: Results of laboratory tests of the material samples [24].

Mean values of laboratory test results	Uniaxial compression strength, R_c	Tensile strength, R_{rb},	Cohesion, c	Angle of internal friction, φ
Material/mine	(MPa)	(MPa)	(MPa)	(°)
Porphyry ZALAS	106.5	5.9	8.6	54.0
Sandstone BRACISZÓW	155.3	8.0	14.5	49.5
Sandstone GUIDO	97.4	6.2	11.9	49.6
Sandstone BRENNA	58.8	3.9	6.0	53.0

Table 2: Number of successful rock loosening attempts.

Material/mine	Number of successful loosening attempts
Porphyry ZALAS	30
Sandstone BRACISZÓW	27
Sandstone GUIDO	36
Sandstone BRENNA	22
	Σ115

3 In situ test results

Solid model of the separated fragment of rock, obtained by 3D scanning, makes it possible to reproduce the outline of the separation path in any cross-section. In order to determine the maximum and minimum loosening range, a cross-section corresponding to these ranges was generated for each solid model. The generated cross-section allowed also for precise determination of the effective anchoring depth. Examples of such cross-sections for different anchoring depths H_{ef} are shown in Figure 11.

As a result of the tests carried out within the RODEST project, 115 successful solid rock loosening trials were made using a fixed undercutting anchor. Number of successful loosening attempts by each mine is presented in Table 2.

3.1 Impact of anchoring depth on the maximum loosening force

Assessment of the impact of effective anchoring depth on the maximum force during loosening was based on a compilation of data collected during the tests. The depth
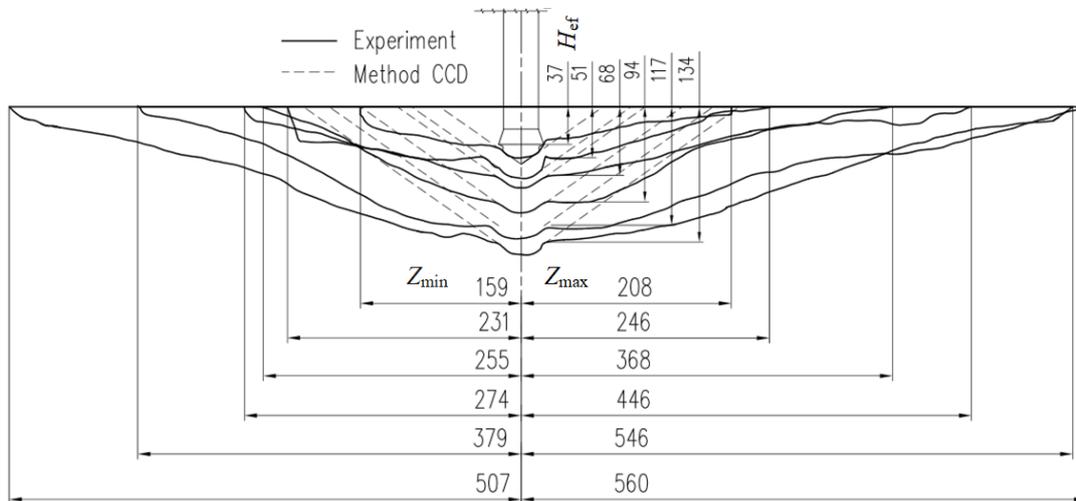
Figure 11: Examples of a cross-sections through a loosened rock, specifying the effective anchoring depth H_{ef}, maximum Z_{max}, and minimum Z_{min} loosening range (on the example of BRENNA mine). CCD, concrete capacity design.
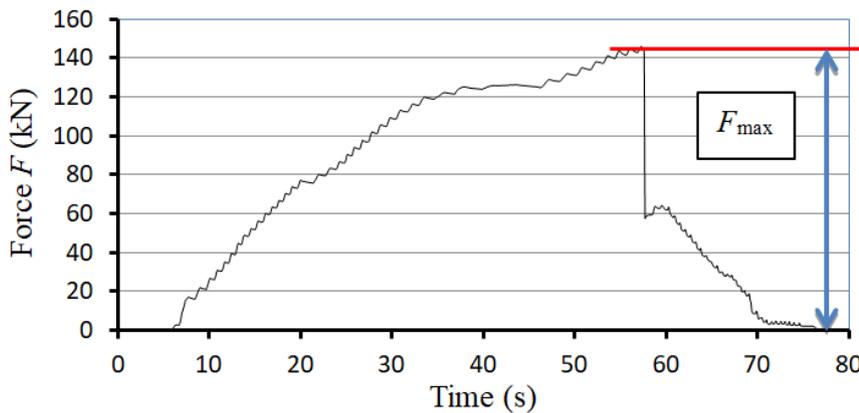

Figure 12: Determination of maximum force F_{max}, recorded during the loosening test.

of effective anchoring H_{ef} was determined from the cross-section of each test (Figure 11). In turn, the maximum force during each loosening test was read out from the force time processes during the loosening test (Figure 12).

On the basis of known effective anchoring depth H_{ef} and the maximum force F_{max}, the specification of all test results was prepared. Presented results of each test were initially approximated by means of a power function divided into each mine (Figure 13). The figure also presents the approximation curve and the R^2 index.

Analyzing the approximating function for each rock type, it can be stated that for each rock, the loosening force increases with the anchoring depth. Exponential function with the exponent close to ~1.6 is the best type of function mapping. The exception is the function describing the test results in the BRACISZÓW mine, with the exponent being

equal to ~1.0. The difference is probably caused by a small number of tests for higher effective anchoring depth H_{ef}. High concentration of measurements was applied within the range of $H_{ef} \sim 30 \div 80$ $H_{ef} = 30-80$.. It was also important to carry out tests on rock blocks taken from different regions of the mine characterized by different mechanical properties.

To compare the test results with the computational model CCD, in Figure 14, the curves drawn using the maximum loosening forces F_{max} determined experimentally (Figure 13) with the anchoring load capacity $N_{u,m}$ calculated from equation (2) were compared. It can be concluded that for all rock types, the calculated anchoring load capacity $N_{u,m}$ was significantly lower than the value calculated from the substitute function F_{max} determined experimentally.
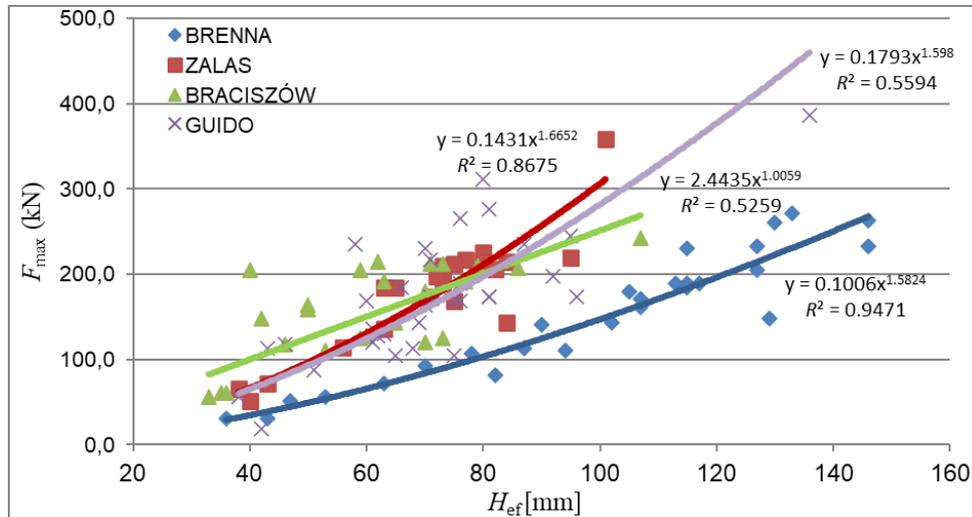
Figure 13: Curves of maximum loosening force F_{max} in relation to the effective anchoring depth H_{ef} for different rock types.
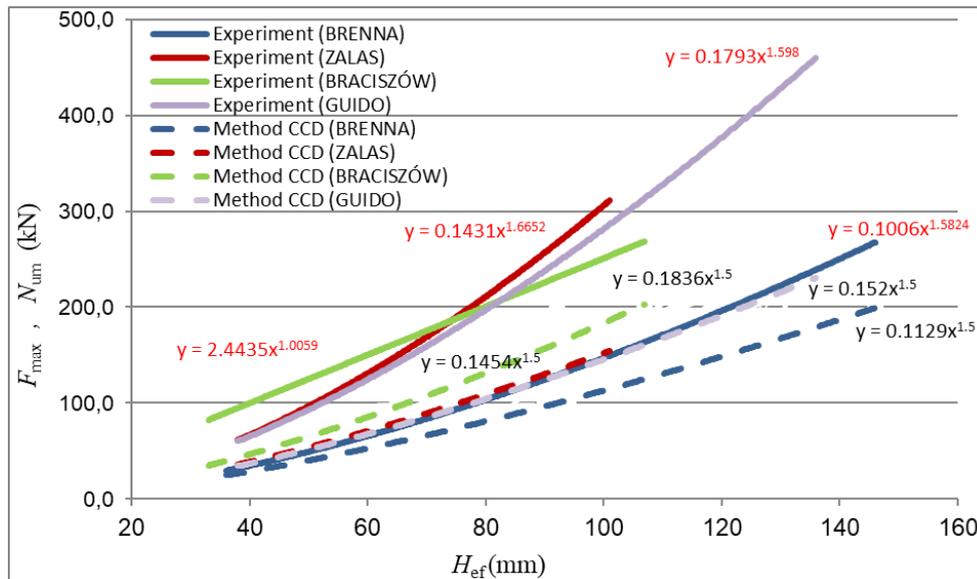

Figure 14: Curves drawn using the maximum loosening forces F_{max} determined experimentally (Figure 13) with the anchoring load capacity $N_{u,m}$ calculated from equation (2).

3.2 Determination of the loosening range

In order to determine the mean values of the loosening range for each test, the maximum Z_{max} and the minimum Z_{min} ranges were defined for each test based on the loosening cross-sectional area (Figure 11), from which the mean arithmetic value $Z_{av.}$ was determined by the following equation:

$$Z_{av.} = (Z_{max} + Z_{min})/2 \qquad (4)$$

Comparison of the mean range values Z_{av} for each measurement depending on the effective anchoring depth H_{ef} is shown in Figure 15.

The average loosening range for each type of rock was approximated by an exponential function. For each type of rock, an increase in the average loosening range which is proportional to the increase in the effective anchoring depth can be observed. Poor matching of the approximating function, especially for the results of tests carried out in the BRACISZÓW and GUIDO mines, is probably associated with the heterogeneity of the rocks in
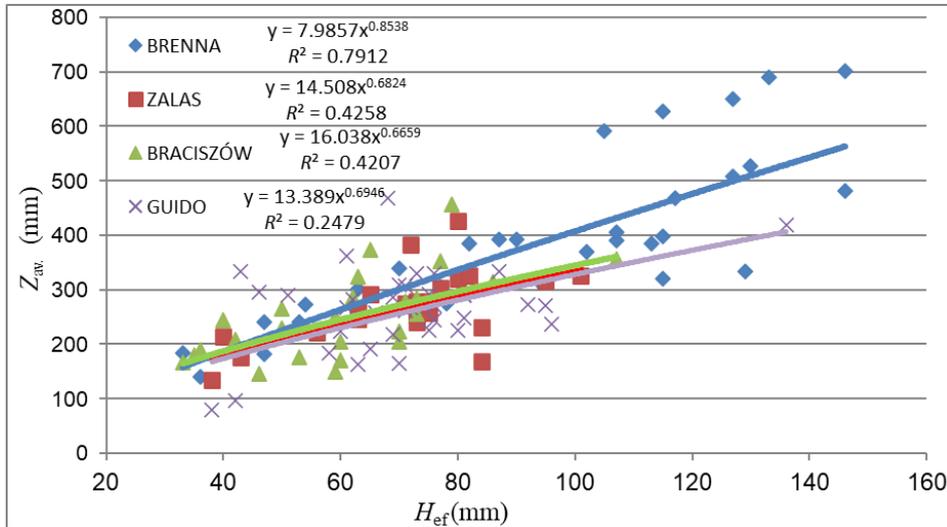
Figure 15: Curves of mean range values $Z_{av.}$ in relation to the effective anchoring depth H_{ef} for different rock types.
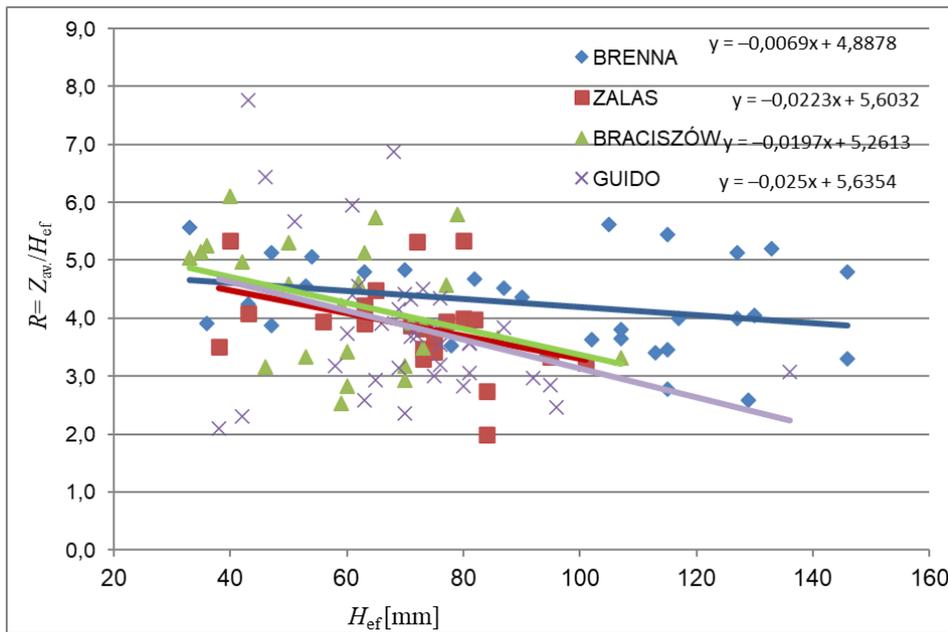

Figure 16: Changes in the coefficient R in relation to the effective anchoring depth H_{ef} for different types of rocks.

Table 3: Average values of R coefficient.

	ZALAS	BRACISZÓW	GUIDO	BRENNA
$R = Z_{av.}/H_{ef}$	3.9	4.1	3.9	4.2

which the tests were conducted. During the tests (especially in these two mines), sometimes a sudden change in the direction of propagation of the loosening gap could be observed in relation to those usually observed. For each test, the coefficient R determining the quotient of the

average loosening range Z_{av} and the effective anchoring depth H_{ef} was determined by the following formula:

$$R = Z_{av}/H_{ef} \qquad (5)$$

In Figure 16, changes in coefficient R in relation to the effective anchoring depth for different types of rock are presented.

The average values of R coefficient for each type of rock within the anchoring depth range 30–150 mm do not differ much and are equal to 3.9–4.2. This is more than twice the
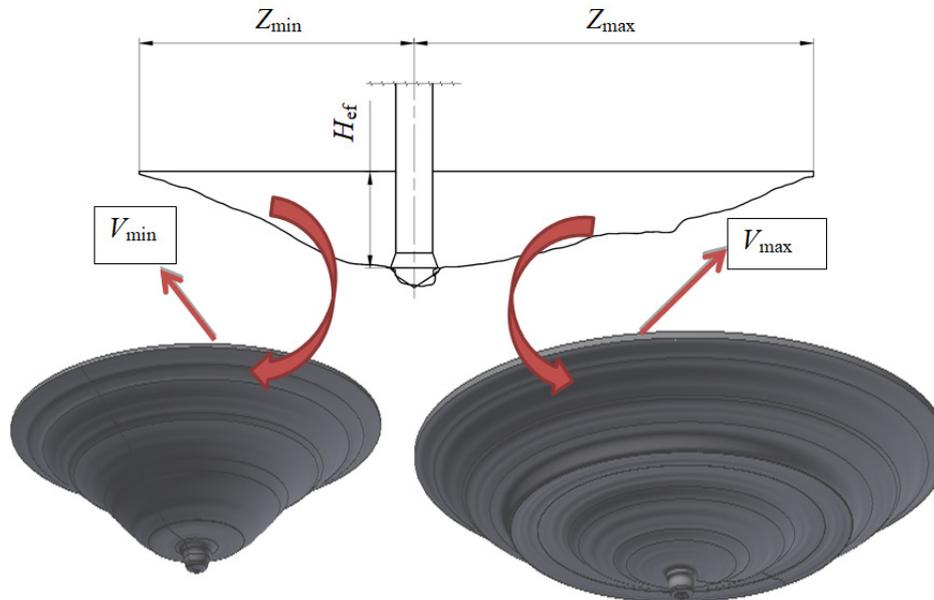
Figure 17: Schematic presentation of the procedure for determination of loosened rocks' surface area and volume.

value used for the calculation of the anchoring capacity (Figure 2). At the same time, one can notice a tendency to reduce the R coefficient together with increase of the effective anchoring depth for all types of tested rocks. These values are presented in Table 3.

3.3 Determination of volume of loosened rock

Fragments of the solid rock loosened using the undercutting anchors have, in most cases, a shape similar to a cone. Anisotropy, internal stratification, or micro-damages in the rock examined can cause that the crack propagation may progress differently in each direction. Thus, the mean value from the maximum and minimum ranges in each test was used to determine the loosening range (equation (5)). A similar analysis was carried out to determine the mean volume after loosening. Solids of revolution were generated for the cross-sections corresponding to the maximum Z_{max} and the minimum Z_{min} ranges of each loosening process. Revolution solids were generated using the specialized CAD software, with the help of which their volumes V_{max} and V_{min} were determined for the solid generated by the range-defined cross-sections Z_{max} and Z_{min}. A schematic presentation of the procedure for their determination is shown in Figure 17.

The mean value of the loosened rock volume for each test was defined as the arithmetic mean value $V_{av.}$, which was determined by the following equation:

$$V_{av.} = (V_{max} + V_{min})/2 \qquad (6)$$

The mean volume $V_{av.}$ for each measurement versus the effective anchoring depth H_{ef} is presented in Figure 18.

Additionally, in Figure 18, the curve referring to the volume of loosened cone calculated for the loosening range equal to $Z=1.5H_{ef}$ of effective anchoring depth (according to the CCD method described by equation (2)). Volume function based on CCD method has the following form:

$$V_{CCD} = 3H_{ef}^{3} \qquad (7)$$

As it can be seen, all functions are converged and have an exponential character. The best function matching is observed for the tests carried out in the BRENNA mine. In addition, the average values of the loosened volume during in situ tests are much higher than the values of the CCD calculation model. It results directly from the fact that the CCD method assumes a much smaller loosening range Z in relation to the average values $Z_{av.}$ observed during tests (Table 3).

4 Conclusions

Analysis of the results of in situ loosening tests carried out so far indicates that the process of rock loosening
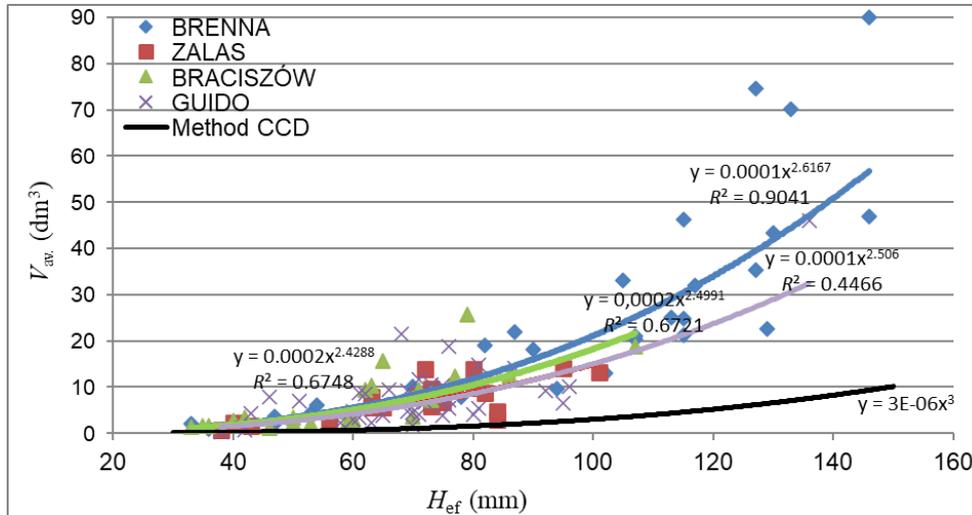
Figure 18: Curves of mean volumes V$_{av.}$ versus the effective anchoring depth H_{ef} for different rock types with the volume function based on CCD method. CCD, concrete capacity design.

using an undercutting anchor is an advantageous method for unconventional mining process. The maximum force Fmax needed to loosen a fragment of solid rock of a shape similar to a cone increases with the depth of effective anchoring Hef and depends on the strength properties of a given type of rock and increases with the increase of strength under uniaxial compression Rc and tension R_r. However, results from the tests conducted show that the average maximum force F_{max} required for loosening rocks of all rock types exceeded the value calculated by the CCD method. It means that CCD computational method is enough for determination of anchor load capacity, but it gives the results not enough for determination of the force required for loosening rock of the cone shape (Figure 14).

Anisotropy, internal stratification, or micro-damage within the mined rock impacts the crack propagation, and thus the loosening range. Therefore, the mean values determined for the maximum and minimum loosening ranges of each test were used for analysis of the range and volume of loosened rocks (Figures 11 and 15). The dimensions of the failure cones with respect to the tested embedment depths and rock substrates observed in this investigation are far above what results from the standard computational models. The ratio of the average Z_{av} and the effective anchoring depth H_{ef} determined by the R coefficient is about 4. This is more than twice the value used for the calculation of the anchor load capacity (Figure 2). Numerical tests indicate that for the assumed mechanical parameters of rock and the depth of undercutting the rock with an anchor (H_{ef}, Figure 11), the angle of the cone failure is approximately 25°, which translates into a factor R=2.1 (equation (2)) . At the same time, the in situ test showed

a tendency to reduce the R coefficient together with increase of the effective anchoring depth for all types of tested rocks. It coincides with the observations presented in the literature ([3], Figure 4c).

The mean volume of loosened cones in in situ conditions determined by a 3D scanner and CAD software is much higher than the theoretical volume calculated by the CCD method (Figure 18); the differences can be even several times higher. Significant differences in the loosened volumes result from the fact that the shape of the loosened material during in situ tests significantly differed from the ideal cone as in the CCD method (Figure 11). Determination of the loosened rock fragments' volume is important in determination of the rock mining efficiency with use of undercutting anchors.

In order to facilitate the use of the method in real conditions, based on the results collected during the tests, it is necessary to build a simplified model of rocks loosening that allows estimation of the loosening strength and range of loosening, depending on the anchoring depth and rock strength, to enable correct selection of the loosening method in mining conditions. It is also important to adapt the numerical simulation method best for the in situ tests.

References

[1] ACI Committee 355. (1991). *State-of-the-art report on anchorage to concrete (ACI 355.1R-91)*. Reapproved 1997. Detroit, USA: American Concrete Institute.

[2] Ashour, A., & Alqedra, M. (2005). Concrete breakout strength of single anchors in tension using neural networks. *Advances in Engineering Software*, *36(2)*, 87-97.

[3] Brincker, R., Ulfkjær, J. P., Adamsen, P., Langvad, L., & Toft, R. (1995). Analytical Model for Hook Anchor Pull-out. In R. Widmann (Ed.), *Proceedings of the International Symposium on Anchors in Theory and Practice: Salzburg, Austria, 9-10 october 1995* (pp. 3-15)

[4] Cebula, D. (2015). Wyniki badań dołowych technologii mechanicznego odspajania skał. In *Nowoczesne metody eksploatacji węgla i skał zwięzłych: Monografia (*The results of underground testing of mechanical rock break technology. *Modern methods of coal and solid rock mining. Monograph. – in polish)* (pp.212-222). Kraków: Akademia Górniczo-Hutnicza im. Stanisława Staszica.

[5] CEN/TC250, "EN1992-4 - Eurocode 2: Design of concrete structures - Part 4: Design of fastenings for use in concrete," 2018.

[6] CEN/TS 1992-4-1: Design of fastenings for use in concrete - Part 4-1: General, CEN, Brussels, 2009.

[7] Comite Euro-International du Beton (CEB). (1994). *Fastenings to concrete and masonry structures*. London, England: Thomas Telford Services Ltd.

[8] Drwięga, A., et. al. (2014). *Sprawozdanie za rok 2014 z realizacji projektu INREQ (Report for 2014 on the implementation of the INREQ project – in polish),*. Unpublished Report. Gliwice: ITG KOMAG.

[9] Fuchs, W., Eligehausen, R., Breen, J.E. (1995). Concrete capacity design (CCD) approach for fastening to concrete. *ACI Structure Journal, 92 (1)*, 73-94.

[10] Gontarz, J., Podgórski, J., Jonak, J., Kalita, M., & Siegmund, M. (2019). Comparison between numerical analysis and actual results for a pull-out test. *Engineering Transactions, 67*(3), 311-331. doi:10.24423/EngTrans.1005.20190815

[11] Gontarz, J., Podgórski, J., Siegmund, M. (2017). *Comparison of crack propagation analyses in a pull-out test: AIP Conference Proceedings*. 1922. doi: 10.1063/1.5019141

[12] Hariyadi, Munemoto, S., & Sonoda, Y. (2017). Experimental analysis of anchor bolt in concrete under the pull-out loading. Paper presented at the Procedia Engineering, , 171 926-933. doi:10.1016/j.proeng.2017.01.391

[13] Hilti. (2014). *Anchor Fastening: Technology Manual*, 09. Retrieved from https://www.hilti.group/content/dam/documents/pdf/a1/singapore/thailand-products-catalog/Thailand-Anchor%20Fastening%20Technology%20Manual-th.pdf

[14] Jonak, J., & Siegmund, M. (2019). FEM 3D analysis of rock cone failure range during pull-out of undercut anchors. Paper presented at the *IOP Conference Series: Materials Science and Engineering, , 710*(1) doi:10.1088/1757-899X/710/1/012046

[15] Jonak, J., Siegmund, M., et al. (2018). *Sprawozdanie z realizacji zadania 2 projektu RODEST (Report on implementation of tasks 2 of the RODEST project – in polish),* Unpublished Research Paper. Gliwice: ITG KOMAG.

[16] Kalita, M., & Prostański, D. (2012). Technologia drążenia tuneli ratowniczych metodą niszczenia spójności skał. (Technology of rescue tunneling by use of rock cohesion damaging method – in polish) *Przegląd Górniczy, 12*. 86-91. 1

[17] Klich, A. Et al. (1998). *Niekonwencjonalne techniki urabiania skał (Unconventional rock mining techniques – in polish)*. Katowice: Wydawnictwo Śląsk.

[18] Nilforoush, R. (2019)- A Refined Model for Predicting Concrete-Related Failure Load of Tension Loaded Cast-in-Place Headed Anchors in Uncracked Concrete. Nordic Concrete Research Volume 60 (2019), (pp. 105-129) doi:10.2478/ncr-2019-0091

[19] Piccinin, R.; Ballarini, R.; Cattaneo, S. Pullout Capacity of Headed Anchors in Prestressed Concrete. *Journal of Engineering Mechanics* 2012, *138*, 877-887.

[20] Siegmund, M., & Jonak, J. (2017). Analiza wyników badań wstępnych oraz określenie kierunku dalszych prac badawczych technologii drążenia tuneli ratowniczych metodą mechanicznego odspojenia. Analysis of the results of preliminary studies and determination of direction of further research work on technology of drilling the rescue tunnels by the method of mechanical loosening - *in polish), Cuprum, 1*, 57-71

[21] Siegmund, M., & Jonak, J. (2019). Analysis of the process of loosening the rocks with different strength properties using the undercutting bolts. Paper presented at the *IOP Conference Series: Materials Science and Engineering, , 679*(1) doi:10.1088/1757-899X/679/1/012014

[22] Subramanian, N. Recent developments in the design of anchor bolts, 7he IndianConcrete Journal, July 2000, Vol. 74, No. 7, pp. 407-414.

[23] Tan, E. L., Varsani, H., Liao, F. Y. (2019). Experimental study on demountable steel-concrete connectors subjected to combined shear and tension. *Engineering Structures*, 183, 110-123. doi: 10.1016/j.engstruct.2018.12.08

[24] Tomiczek, K. (2017-2018). *Badania wytrzymałościowe wybranych skał magmowych i osadowych: Raporty z badań dla ITG KOMAG (Strength tests of selected igneous and sedimentary rocks. Research reports for ITG KOMAG – in polish)* (NB-363/RG4/2017, NB-11/RG4/2017, NB-117/RG4/2018, NB 266/RG-4/2018). Unpublished Research Reports. Gliwice: Politechnika Śląska.